Molecular Crystal Global Phase Diagrams II: Prototypical crystal packings for group T_d molecules

J. Brandon Keith* and Richard B. McClurg

Department of Chemical Engineering and Materials Science,

University of Minnesota, Minneapolis, Minnesota

Abstract

Previously [1, 2], we developed a method for constructing global phase diagrams for molecular crystals in which crystal structure is presented as a function of intermolecular potential parameters. These diagrams are useful for crystal design and reverse engineering the intermolecular potential of an experimentally observed crystal structure. We use this previous method to reverse engineer a potential sufficient to produce the structures of fully ordered single component crystals composed of tetrahedral molecules in the Cambridge Structural Database. This is significant because our prior work did not specify the number of different molecular packings, called reference lattices, to consider. Nor did it specify the number of parameters needed for the diagrams. We find the structures of all tetrahedral molecules pack in 15 reference lattices: bcc (25.7%), fcc (24.3%), A5 (8.6%), hcp (8.6%), sc (8.6%), and others (24.2%).

*Electronic address: jbrkeith@gmail.com; Also at Department of Physics and Astronomy, Brigham Young University, Provo, Utah

I. INTRODUCTION

Previously, we introduced a tool for exploring the molecular parameter space of plastic and molecular crystals using a global phase diagram (GPD) [1, 2]. Global phase diagrams summarize the phase behavior of a class of substances as a function either of parameters in an empirical equation of state or of parameters in an intermolecular potential. The classic example of a GPD of the first type is the classification scheme for high pressure vapor liquid phase equilibria by van Konynenburg [3]. Their classification was based on the van der Waals equation of state with simple binary mixing rules. Despite the crude equation of state employed, it is still widely used to classify the phase behavior of real binary mixtures. Our GPD's are of the second type. They use an intermolecular potential constructed from a complete set of basis functions for rotational space for all molecules of a particular point group and a set of molecular center-of-mass packings inferred from experimental crystal structures. The parameters of the intermolecular potential become axes on GPD's for each packing and the crystal structures are phase regions in the diagrams.

An important benchmark of GPD's utility is to show that experimentally observed structures can be found and their intermolecular potential parameters read from the axes. Our goal is to determine the number of translational packings, or reference lattices, required in GPD construction and the number of potential parameters needed to find all experimental phases. A small number of each will disprove previous hypotheses that many parameters are needed [4] and enhance the useability of GPD's in materials design.

The outline of the balance of the paper is as follows. In Sec. II we discuss the derivation of our data set, its chemical and crystallographic characteristics, and group entries based on structural similarity. In Sec. III we deduce reference lattices for each structure by pseudo-symmetry detection and describe the fit of the structures to these lattices. In Sec. **??** we review the rotational potential and outline the computational procedure to find the potential parameters for each structure. In Sec. IV we discuss and visualize the reverse-engineered potentials for tetrahedral molecules in the CSD and discuss features and limitations of the model.

II. EXPERIMENTAL DATA SET

Since our molecular crystal global phase diagrams are constructed for molecules of a given molecular point group symmetry, we have chosen to use the *CSDSymmetry* database as our primary source of crystal structures [5]. This database summarizes the point groups of molecules that form error-free, nonpolymeric, nonionic, coordinate-determined molecular crystals in the CSD. Duplicates were removed from the database and hydrogen atoms were not considered when assigning point groups. While the methods introduced in our previous work [2] are applicable to disordered structures, which are systematically absent from *CSDSymmetry*, it is a convenient source of crystal data for molecules of a particular point group. Our methods are restricted to single component crystals, however. Therefore we worked with the single component crystal subset of the *CSDSymmetry* database. This was accomplished by first querying the CSD for all single component crystals using CONQUEST, the interface to the CSD, and then using CONQUEST to take the intersection of the two data sets.

Continuing the example begun in our prior work [2], we chose to consider crystals composed of molecules with T_d molecular point group symmetry. We have augmented the data from *CSDSymmetry* with a recently determined structure of the low temperature ordered phase of heavy methane [6]. The data set contains 71 crystal structures of 70 different chemical substances. Only carbon tetrachloride (CCl_4) appeared twice in different polymorphs. [CSD structures CARBTC [7] and CARBTC07 [8]]. Names and chemical formulas for all the entries are given in Table I. The chemical structures include 15 hydrocarbons and their substituted derivatives and 56 organometallics. The organometallics contain 30 different metals: Al, As, Bi, Cd, Co, Cs, Cu, Ga, Ge, Hf, In, Mg, Mn, Na, Ni, Np, Pb, Pt, Re, Rh, Ru, Sb, Si, Se, Sn, Tc, Th, Ti, U, and Zn. Eight types of molecular frameworks are present in the data set: Cubane (29), Adamantane (17), MX_4 (16), Tetrahedrane (3), and others (6). There are entries from all seven crystal systems in the data set. Twenty crystals are cubic (or isometric), one is hexagonal, five are trigonal, ten are tetragonal, six are orthorhombic, 22 are monoclinic, and seven are triclinic as shown in Fig. 1. This distribution is different than the CSD as a whole [9], but that is not surprising given the larger-than-average number of symmetries in the T_d point group. The data set is sufficient however to test whether molecular crystal global phase diagrams apply to hydrocarbons and organometallics, a variety of

molecular frameworks, and all seven crystal systems.

One entry [CSD structure XUWROW [10]] is a very unusual structure containing 70% voids as recorded by the CCDC staff in its cif file in the CSD, presumably using the standard van der Waals radii in the documentation of CCDC software [11]. It was grown as a thin epitaxial crystal under ultra-high vacuum. Apparently the crystal structure is strongly influenced by the substrate and we exclude it from further consideration.

The remaining crystal structures were organized into groups that bear a strong "structural relation" as discussed in the International Tables for Crystallography (ITC) [12]. For crystals to belong to the same group they must have the same space group symmetry, cell lengths in similar proportions, similar cell angles, and molecular centers at equivalent Wyckoff point(s) with similar structural parameter values where applicable. We refer to these groups as sharing a particular distinct structure. Note that we do not require that the atomic positions be similar to be classified in the same distinct structure. For example, two structures [CSD structures DILWIE01 [13] and ZEYHIU [14]] crystallize in space group 165 with molecules at Wyckoff point d. Their cell parameters are also in similar ratios. Therefore, we classify them in the same distinct structure, despite their different chemical structures with different numbers of atoms.

Two structures in *CSDSymmetry* [CSD structures HMGETP [15] and JUFWUC [16]] have molecules that are tetrahedral within the default error bounds for detecting molecular symmetry, but are sufficiently distorted to influence their space group classifications (195a and 197a, respectively). Either the molecules are very slightly distorted in the crystal or the crystal symmetries are under-specified and actually belong to space groups 215 and 217, respectively. Although slight distortions could result from crystal Jahn-Teller distortions, for example, we adopt the later interpretation. Therefore these crystals have been grouped with distinct structures 215a and 217a, respectively. This assignment is discussed from an energetic point of view in Sec. IV.

The 70 crystal structures fell into 46 distinct structures. Five structures are cubic (or isometric), one is hexagonal, four are trigonal, eight are tetragonal, six are orthorhombic, sixteen are monoclinic, and six are triclinic. These distinct structures are further characterized in the following section.

III. REFERENCE LATTICE ASSIGNMENTS

Our global phase diagrams are constructed starting with a fully disordered plastically crystalline reference state. At sufficiently high temperature the intermolecular potential, which hinders free rotation, becomes weaker than the thermal energy. In this limit molecules are free to disorder and ultimately to freely rotate. Since the molecules are disordered they may occupy high symmetry Wyckoff points in high symmetry space groups. These are space groups with special values of the cell parameters $(a, b, c, \alpha, \beta, \gamma)$ and molecules located at special values of the unit cell fractional coordinates (x,y,z). Each molecule has four or more generally equivalent non-coplanar nearest neighbors. This is needed for structural stability in three dimensions. We call these reference lattices.

High symmetry reference lattices may be determined for an experimental crystal structure by determining the space group formed from the lattice of the molecular centers of mass. These calculations were done using FINDSYM in the ISOTROPY software suite [17] with coordinates scaled by the minimum unit cell length $\{a, b, c\}$ and a large error tolerance setting (0.1). Initially it may seem unexpected that molecular crystals, the majority of which belong to monoclinic or triclinic space groups [18], should be slight distortions of high symmetry lattices. However, prior work in this area has shown this is not only possible but quite common [19, 20]. Standard unit cell choices for low symmetry crystals systems often hide the similarity of a suitably-chosen supercell to a reference lattice in a higher symmetry crystal system. This high translational symmetry is a result of the close-packing tendency of molecules. Broken symmetries are due to orientational ordering and anisotropic intermolecular potentials.

Occasionally a structure arises with fewer than four nearest neighbors per molecule. Due to the inherent lack of structural stability of this arrangement, this suggests the crystal is in fact a lattice of molecular clusters, typically *dimers*, acting as a single entity. In such a case the center of mass of the dimers is used in FINDSYM again with a larger error tolerance.

Given a list of common reference lattices, we developed an automated technique to identify the reference lattices of experimental structures. From a list of possible reference lattices, we superimpose an experimental structure on each possible lattice so one molecule in each structure overlaps. Then the experimental structure is rotated and isotropically scaled in order to minimize the sum of the absolute values between the center of each molecule of the

experimental structure and the center of the closest reference lattice molecule,

$$\min_{a,\boldsymbol{\omega}} \sum_m |\boldsymbol{R}(a,\boldsymbol{\omega}) \cdot \boldsymbol{X}_m^{\text{exp}} - \boldsymbol{X}_{\text{closest}}^{\text{ref}}|, \tag{1}$$

where $\boldsymbol{R}(a,\boldsymbol{\omega})$ is a Cartesian rotation matrix multiplied by an isotropic scaling factor a (Appendix A), $\boldsymbol{X}_m^{\text{exp}}$ is the center of mass of a molecule in the experimental structure, $\boldsymbol{X}_{\text{closest}}^{\text{ref}}$ is the center of mass of the closest molecule in one of the possible reference lattices, and m sums over all molecules in the experimental structure, which is typically limited to the first 14 neighbors of the superimposed center molecule. This cutoff is justified by CSD studies [21] showing 14 to be the most common molecular coordination number. This technique was used in a computer program to identify the majority of the fcc, bcc, hcp, sc, and diamond reference lattices.

Applying these techniques to our data set gives the reference lattice assignments in Tables II- VI. Generally we name reference lattices first by their common name (*i.e.* fcc) if available, then by their Strukturbericht designation (*i.e.* A15) if available, and then by their space group/filled Wyckoff positions if necessary (*i.e.* 70a). The raw atomic positions, symmetry operators, etc. contained in the cif and fdat data files from the CSD were processed using the cctbx collection of algorithms [22]. Algorithms from the ISOTROPY software suite [17] and the Bilbao Crystallographic Server [23] were also used to identify group-subgroup relations, track Wyckoff point evolution, etc. In the following subsections we review the reference lattices for the structures in the experimental data set.

A. Cubic (Isometric) Space Groups

The cubic crystal structures are summarized in Table II. Each structure is listed as a space group number followed by its occupied Wyckoff points. A representative of each structure is named in the next column. Under each representative structure is the reference lattice. In the third column is shown the ratio $|G|/Z$. This is the number of symmetry operations $|G|$ per molecules in the unit cell Z. We call this ratio the symmetry density of a crystal structure. Defined in this way, the symmetry density is independent of the choice of unit cells. For instance the primitive and conventional fcc cells both have $|G|/Z = 48$. The symmetry density is a maximum of 48 for fcc, bcc, and sc sphere packings. Symmetry breaking, by loss of a class of symmetry operations and/or loss of translations, reduces the

symmetry density. The index $[i]$ of a group-subgroup relation is the ratio of $|G|/Z$ of the group and its subgroup. Thus, the geometric interpretation of the index is the amount by which the symmetry of the crystal is diluted by symmetry breaking (ITC, p726) [12]. The number of entries bearing a strong structural similarity to the representative is shown in the fourth column. For example, structure 217a has space group 217 with molecules situated at Wyckoff point a. Its representative is DEQPAQ and in a disordered state the crystal has the bcc symmetry or reference lattice. Its symmetry density is 24 and that of its reference lattice 48. Therefore, its index in bcc is 2. There are 11 tetrahedral molecular crystals in *CSDSymmetry* with this structure.

The 20 crystal structures in Table II fall into five distinct structural types listed in order of decreasing symmetry density. Structure 227a is unique in that the Wyckoff point symmetry in the reference lattice is consistent with T_d molecular point group symmetry. Therefore the (ordered) experimental structure has the full symmetry of the (disordered) reference lattice. Structures 217a and 215a are subgroups of bcc and sc, both of index two. The molecular symmetry (T_d) is a subgroup of the Wyckoff site symmetry in the reference lattice (O_h). Thus the crystal symmetry is reduced by molecular ordering. Structure 218a,c is similarly a subgroup of index two of A15, but the molecules on the two occupied Wyckoff sites are inequivalent, even in the reference lattice. For each of the preceding structures, there are no arbitrary cell parameters or structural parameters. Thus the molecular centers of mass coincide exactly with the reference lattice.

Structure 205c has one arbitrary parameter, x, for its occupied Wyckoff point. This is called a Wyckoff structural parameter. Figure 2 shows the neighbor distances as a function of the structural parameter. The representative experimental structure [tetracarbonyl-nickel CSD structure FOJBUB02 [24]] has molecules at Wyckoff point c with a structural parameter $x = 0.122$ which is approximately midway between the sc limit ($x = 1/4$) and a doubly occupied fcc limit ($x = 0$ or $1/2$). It is evident from the figure that the crystal structure is equivalent for structural parameters x and $1/2 - x$. Since the neighbor distances at the experimental values of the structural parameter are qualitatively different than in the sc lattice, the simple cubic reference lattice is not acceptable for our purposes. The crystal is best viewed as a dimer packing with dimer centers of mass on an fcc lattice as shown in Fig. 3 for a dimer situated on the $(1/2, 1/2, 0)$ fcc coordinate. Its three-fold axis is parallel to the body diagonal direction. The dimer has point group symmetry D_{3d} so we would expect

to identify this structure on a D_{3d} global phase diagram using an fcc reference lattice. This possibility is not pursued further here.

B. Hexagonal and Trigonal Space Groups

The six structures with hexagonal or trigonal space groups fall into five structural types summarized in Table III. The c/a ratio is given for the experimental lattice in the third column. The c/a ratio for the reference lattice is also given. These are the ratios of the experimental structure embedded in the reference lattice. Thus c/a=1.22 for the bcc reference lattice row of the TCYMET structure entry is not c/a of the bcc crystal but c/a of TCYMET embedded in the bcc reference lattice. This embedding is shown in Fig. 4 in which the lattice constant of the bcc crystal, a', is compared to the lattice constants a and c of TCYMET. In each case in Table III the arbitrary parameters differ by only a few percent from the ideal reference lattices. All five reference lattices are sphere packings (hcp, bcc, or fcc).

In contrast to the cubic lattices, all of the hexagonal and trigonal structures in the data set have molecules at Wyckoff points with variable Wyckoff structural parameters, so their value is given in the fourth column. Below these are shown the structural parameters of the reference lattices. Again the agreement between the translational arrangements of molecules in a crystal with a high-symmetry reference lattice is quite good.

C. Tetragonal Space Groups

Tetragonal structures are summarized in Table IV. We adopt the unique c-axis orientation for tetragonal space groups. The ten structures fall into eight structural types. Structure 142a contains eight molecular centers in the unit cell. Their molecular centers differ by only 1% from two conventional fcc cells stacked in the z-direction. The other structures are less trivially related to their reference lattices and are tetragonally distorted to various degrees.

With the exception of structure 142a, discussed above, each of the tetragonal structures is a sub-group of structures 141a, 139a, or 123a. Figure 5 gives the neighbor distances for tetragonal distortions of these lattices. Note that there is a tetragonal distortion that transforms fcc and bcc into one another. As a result, structures 137b, 121a, 142a, 114a, and

88f could not be uniquely assigned to a reference lattice solely based on their group/subgroup relationships. For these structures, the c/a ratio provides the requisite additional information. The experimental c/a ratios are marked with circles in Fig. 5. There appear to be fewer than nine circles in the figure because several of them overlap. Note that the experimental structures cluster around the sphere packings (marked with dashed lines) or distorted lattices with equidistant neighbors (marked with dotted lines). For instance, the diamond lattice can be tetragonally distorted to yield six equidistant second-nearest neighbors (A5′ in Fig. 5 for $c/a = 2/\sqrt{7}$) or eight equidistant nearest neighbors (A5″ in Fig. 5 for $c/a = 2\sqrt{3}$). The Aa reference lattice is a distorted bcc structure and has ten equidistant nearest neighbors for $c/a = \sqrt{2/3}$. The A6 reference lattice at $c/a = \sqrt{6}$ is a reference lattice for other molecules discussed in later sections. Also there is an additional dimer structure, 88f, among them.

D. Orthorhombic Space Groups

Orthorhombic structures are summarized in Table V. We have adopted the C-centered setting for end centered unit cells. Each of the six structures constitutes its own distinct structural type. Two structures, 64d,f and 60c,d very nearly match the fcc and bcc reference lattices respectively. Structure 19a is identified with the 63c reference lattice which is an orthorhombic structure with 10 nearest neighbors and equal c and a lengths. The b/a=b/c ratio is $\sqrt{5+2\sqrt{6}}$ and the structural parameter for Wyckoff point c (0,y,1/4) is $y = (\sqrt{6} - 1)/4$. The small discrepancies in the 19a x and y structural parameters in this case indicate that the molecules have further relaxed from their reference lattice locations. The three structures in space group 62 provide additional challenges, discussed below.

Whereas the structures in the data set from the higher crystal classes are uniquely identified by their space group and Wyckoff point(s), there are three distinct orthorhombic structures in space group 62 with molecules at Wyckoff point c. Therefore, 62c is insufficient as an identifier for these structures. Since there are two arbitrary cell length parameters and two structural parameters for 62c, it is impractical to plot the neighbor distances as a function of arbitrary parameters as in Fig. 5. Instead we note that Wyckoff point c in space group 62 has four equivalent positions, two at $y = 1/4$ and two at $y = 3/4$. Therefore we view the 3-dimensional structure as a set of layers in the xz-plane uniformly stacked in the

y-direction. Then the c/a ratio and the structural parameters determine the symmetry of the layers. CSD structure GUTCED [25] is composed of alternating layers that are nearly on a square lattice. Based on the stacking of these layers this is a slightly distorted fcc lattice. CSD structure RIMMOP [25] has alternating rectangular layers, which is more similar to the bcc reference lattice. The layers in CSD structure JEYSEL are nearly hexagonal and stacked vertically, rather than alternating. Therefore, it is associated with the simple hexagonal (sh) reference lattice. Thus the three structures in space group 62 are associated with different reference lattices.

E. Monoclinic Space Groups

Monoclinic structures are shown in Table VI. We adopt the unique b-axis orientation, cell choice one, origin choice two, and C centering for end centered lattices. All three lattice parameters and one lattice angle are able to relax so we indicate the closeness of the match for b/a, c/a, and β. The 22 structures fall into 16 distinct structural types. In dividing into these types it is important to note that monoclinic space groups have multiple nonstandard settings. Also, during symmetry breaking from a high-symmetry parent phase to a monoclinic child phase, multiple domains may form creating unit cells that at first examination appear to be dissimilar. An example is CSD structure REKYUB and CSD structure BOGMEP. In a standard setting the important unit cell parameters are $(b/a, c/a, \beta) = (0.48, 1.00, 123)$ and $(0.28, 0.55, 145)$, respectively. The molecular positions also appear different. However, these are simply different domains of the same symmetry-breaking pathway with equivalent unit cell specifications. The phase transition is governed by the same IR, L_3^-, and order parameter direction, P7, using the notation of Stokes and Hatch [17]. Thus we group them in the same structural class.

Monoclinic structures have a greater diversity of reference lattices although those of 9 of the 16 structures are still canonical sphere packings. A good example of this hidden order in these low-symmetry groups is 15f,f,f,f which has 32 molecules per unit cell and four molecules per asymmetric unit, but still nearly packs in an fcc lattice.

Many of the structures belong to the same space group but have different spatial arrangements and so are grouped differently. This is particularly apparent for space groups 14 and 15, two of the most populous space groups in the CSD. A5′, the distorted diamond lattice,

fits two of the monoclinic structures, and simple hexagonal two more. One new packing, 70, is an orthorhombic distorted diamond lattice and has eight molecules at Wyckoff point a. The other new packing, 136, is a tetragonal structure with dimers of molecules at Wyckoff point f. Three additional dimer structures (TMSIAD, CAMPOV, MXSNOX) have dimers centered at high symmetry Wykcoff points without structural parameters.

F. Triclinic Space Groups

Triclinic structures are shown in Table VII. All lattice parameters are variable and are listed. The six structures fall in seven distinct structural types with four reference lattices. There are two new reference lattices. A6 is a tetragonal distortion of fcc discussed in Sec. III C and shown in Fig. 5. Ai is a rhombohedral distortion intermediate between sc and bcc. Its primitive cell a, b, and c parameters are all the same length and $\cos(\alpha) = cos(\beta) = cos(\gamma) = -1/4$. Two dimer structures in 136 and Ai also exist, the latter with dimer complexes at a high symmetry Wyckoff point so no structural parameters are listed in Table VII for XAGXAE.

G. Reference Lattice Summary

The results of the reference lattice assignments of the experimental structures are summarized in Table VIII. The Strukturbericht designation [26], Pearson symbol [27], and common name are shown when known for each reference lattice. The Strukturbericht designations beginning with an A indicate the reference lattices are also the crystal structures of various elements. The space group, occupied Wyckoff positions, and percentage of experimental structures that pertain to each lattice are also shown.

The fit of each experimental structure to its reference lattice is summarized in Fig. 6. In each box the experimental lattice vectors, angles, or Wyckoff positions are compared with their idealized values when inscribed in the corresponding reference lattice. These figures are a visual summary of Tables II-VII. If the fit were perfect all data points would lie directly on the line. The fit is quite good indicating that most low symmetry molecular crystals have molecules situated at or near lattice sites of high symmetry space groups. In the inorganic crystal structure database (ICSD), which is largely composed of atomic crystals,

the most numerous structures are fcc, bcc, hcp, etc. [28] Originally this was considered to be distinct from the CSD which had primarily monoclinic and triclinic structures. Figure 6 challenges this distinction by showing molecular centers of mass, however, are nearly situated on lattice points of these archetypical high symmetry lattices so prevalent in the ICSD. The comparative number of monomer and dimer structures is shown in Fig. 7 as is the breakdown of each into types of reference lattices. It is apparent that although there are 15 reference lattices, 76% of the structures are well represented by only 5 reference lattices.

The dimer structures, reference lattices, and dimer complex point group symmetries are listed in Table IX. Such structures can usually be identified by examining nearest neighbor distances. The presence of three or fewer nearest neighbors is evidence of dimerization. Many of the structures form D_{3d} or nearly D_{3d} dimers as illustrated in Fig. 3, the one exception being CSD structure LUFYEQ [29] whose molecules form C_{2v} complexes.

With the three techniques we have introduced here, (1) dimer screening by nearest neighbor inspection, (2) reference lattice assignment by large tolerance molecular center symmetry determination, (3) reference lattice recognition through template matching, one may determine translational packings or reference lattices for all structures in the CSD. While the second step has generally been done by hand, the first and third step have been automated in Python and MATHEMATICA scripts and are available upon request.

IV. DISCUSSION AND CONCLUSION

A. Reference Lattices

We have shown that all of the single-component tetrahedral molecules in the CSD can be related to a reference lattice, or a high-symmetry starting point for GPD calculations. These reference lattices are generally high symmetry sphere packings or distortions thereof. These results also show the centers of mass of molecular crystals are not structurally distinct from atomic crystals, which also pack in high symmetry sphere packings such as fcc, bcc, hcp, sc, and so on [28]. From our experiences with tetrahedral molecules we hypothesize that the prevalence of low symmetry space groups for molecular crystals in the CSD [30] is due to the orientational ordering of molecules whose centers of mass are close to the lattice points of a higher symmetry space group. This reflects the close packing tendency of molecules [31].

We have shown many structures in our data set can be related to dimers situated on a high symmetry lattice. Understanding the prevalence of dimer structures in the CSD is important when designing configurational search algorithms for crystal structure prediction.

Overall, we have seen most crystal structures in our data set belong to only a few translational packings, or reference lattices. This greatly simplifies the process of constructing GPDs as it diminishes the number of diagrams necessary to describe crystallographic structural space for a given point group of molecules.

B. Conclusions

We have shown that a molecular crystal global phase diagram (GPD) can summarize the experimental data using a modest number of reference lattices and IP parameters. In previous work [1, 2], we somewhat arbitrarily chose a single reference lattice (fcc) and truncated the intermolecular potential with three terms to illustrate the method. Here, we have used an experimental data set of crystals of tetrahedral molecules to determine reference lattices and an IP truncation sufficient to produce the observed phases. The data set is diverse enough to test the GPD's ability to classify a wide range of space groups using a common intermolecular potential. Just as the van Konynenburg global phase diagram classification based on the simple van der Waals equation of state is nonetheless widely used to classify the phase behavior of real binary mixtures, molecular crystal global phase diagrams may be useful in elucidating phase behavior of a variety of real substances and, in turn, used to develop novel intermolecular potentials and materials.

APPENDIX A: CARTESIAN ROTATIONS

The cartesian rotation matrix,

$$\boldsymbol{R}(a,\boldsymbol{\omega}) = a \begin{pmatrix} \cos(\alpha)\cos(\beta)\cos(\gamma) - \sin(\alpha))\sin(\gamma) & -\cos(\gamma)\sin(\alpha) - \cos(\alpha)\cos(\beta)\sin(\gamma) & \sin(\beta)\sin(\gamma), \\ \cos(\beta)\cos(\gamma)\sin(\alpha) + \cos(\alpha)\sin(\gamma) & \cos(\alpha)\cos(\gamma) - \cos(\beta)\sin(\alpha)\sin(\gamma) & \\ -\cos(\gamma)\sin(\beta), & & \end{pmatrix}$$

$$\left.\begin{array}{c}\cos(\alpha)\sin(\beta)\\ \sin(\alpha)\sin(\beta)\\ \cos(\beta)\end{array}\right) \tag{A1}$$

is produced by converting spherical coordinate Wigner functions to cartesian coordinates.

ACKNOWLEDGMENTS

This work received financial support from the American Chemical Society - Petroleum Research Fund (PRF #41774-AC10). Computational resources maintained by the University of Minnesota Supercomputer Institute were used for portions of this research.

---

[1] J. B. Keith, J. A. Mettes, and R. B. McClurg, Crystal Growth and Design **4**, 1009 (2004).

[2] J. A. Mettes, J. B. Keith, and R. B. McClurg, Acta Cryst. A **60**, 621 (2004).

[3] P. H. van Konynenburg and R. L. Scott, Philos. Trans. R. Soc. London, Ser. A **298**, 495 (1980).

[4] W. J. Briels, J. Chem. Phys. **73**, 1850 (1980).

[5] J. W. Yao, J. C. Cole, E. Pidcock, F. H. Allen, J. A. K. Howard, and W. D. S. Motherwell, Acta Crystallogr. B **58**, 640 (2002).

[6] M. A. Neumann, W. Press, C. Noldeke, B. Asmussen, M. Prager, and R. M. Ibberson, J. Chem. Phys. **119**, 1586 (2003).

[7] G. Piermarini and A. Braun, J. Chem. Phys. **58**, 1974 (1973).

[8] S. Cohen, R. Powers, and R. Rudman, Acta Cryst. B **35**, 1670 (1979).

[9] W. H. Bauer and D. Kassner, Acta Cryst. B **48**, 356 (1992).

[10] M. Sung, G. Kim, J. Kim, and Y. Kim, Chem. Mater. **14**, 826 (2002).

[11] I. J. Bruno, J. C. Cole, P. R. Edgington, M. K. Kessler, C. F. Macrae, P. McCabe, J. Pearson, and R. Taylor, Acta Cryst. B **58**, 389 (2002).

[12] T. Hahn, ed., *International Tables for Crystallography* (D. Reidel Pub. Co., Boston, 1983).

[13] K. H. Ebert, W. Massa, J. Donath, H. Lorberth, B. S. Seo, and E. Herdtweck, J. Organomet. Chem. **559**, 203 (1998).

[14] H. Noth and M. Thomann, Chem. Ber. **128**, 923 (1995).

[15] A. R. Dahl, A. D. Norman, H. Shenav, and R. Schaeffer, J. Am. Chem. Soc. **97**, 6364 (1976).

[16] K. F. Tesh, B. D. Jones, T. P. Hanusa, and J. C. Huffman, J. Am. Chem. Soc. **114**, 6590 (1992).

[17] H. T. Stokes and D. M. Hatch, *Isotropy*, stokes.byu.edu/isotropy.html (2002).

[18] P. Simon, J. Bassoul, *Design of Molecular Materials: Supramolecular Engineering* (John Wiley and Sons, New York, 2000).

[19] W. D. S. Motherwell, Acta Crystallogr. B **53**, 726 (1997).

[20] S. Reichling and G. Huttner, Eur. J. Inorg. Chem. **56**, 857 (2000).

[21] E. Peresypkina and V. Blatov, Acta Cryst. B **56**, 501 (2000).

[22] R. Grosse-Kunstleve, N. Sauter, N. Moriarty, and P. Adams, J. Appl. Cryst. **35**, 126 (2002).

[23] E. Kroumova, M. I. Aroyo, J. M. Perez Mato, A. Kirov, C. Capillas, S. Ivantchev, and H. Wondratschek, Phase Transitions **76**, 155 (2003).

[24] D. Braga, F. Grepioni, and A. G. Orpen, Organometallics **12**, 1481 (1993).

[25] J. E. Dahl, S. G. Liu, and R. M. K. Carlson, Science **299**, 96 (2003).

[26] A. J. C. Wilson, ed., *Structure Reports for 1947-1948* (N.V.A. Oosthoek's Uitgevers, Utrecht, 1951).

[27] W. B. Pearson, *A Handbook of Lattice Spacings and Structures of Metals and Alloys* (Pergamon Press, New York, 1967).

[28] A. D. Mighell and J. R. Rodger, Acta Cryst. A **36**, 321 (1980).

[29] B. Wrackmeyer, W. Milius, and A. Badshah, J. Organomet. Chem. **656**, 97 (2002).

[30] F. H. Allen and W. D. S. Motherwell, Acta Cryst. B **58**, 407 (2002).

[31] A. I. Kitaigorodskii, *Organic Chemical Crystallography* (Consultants Bureau, New York,

1961).

TABLE I: Identifiers, chemical formulas, and names of the tetrahedral data set.

Identifier	formula	name	frame
ADAMAN08	C10 H16	Adamantane	adam
BASXOI	C4 H12 Se6 Sn4	1,3,5,7-Tetramethyl-2,4,6,8,9,10-hexaselena-1,3,5,7-tetrastanna-adamantane	adam
BOGMEP	C24 H48 Cl6 Cu4 N16 O1	hexakis(M_2-Chloro)-(M_4-oxo)-tetrakis(hexamethylenetetramine-copper(ii))	other
CAMPOV	C16 H36 N4 Sn4	tetrakis((M_3-t-Butylimino)-tin)	cuban
CANFIG	C4 H24 B4 U1	tetrakis(Methyltrihydroborato)-uranium(iv)	MX_4
CANFOM	C4 H24 B4 Th1	tetrakis(Methyltrihydroborato)-thorium(iv)	MX_4
CARBTC	C1 Cl4	Carbon tetrachloride	MX_4
CARBTC07	C1 Cl4	Carbon tetrachloride	MX_4
CTBROM	C1 Br4	Carbon tetrabromide	MX_4
CUCZUV	C20 H36	Tetra-t-butyltetrahedrane	tetra
DEQPAQ	C36 H100 B4 N12 Na4	tetrakis((M_3-Tetrahydroborate-H,H,H)-pentamethyldiethylenetriamine-sodium)	other
DILWIE01	C16 H48 Pt4 S4	tetrakis((M_3-Methylsulfido)-trimethyl-platinum(iv))	cuban
DOCNIS	C8 H12 S6	1,3,5,7-Tetramethyl-2,4,6,8,9,10-hexathia-adamantane	adam
FOHCUA	C12 Ni4 O18 P4	P,P',P",P"'-tetrakis(Tricarbonyl-nickel)-tetraphosphorus-hexaoxide	adam
FOJBUB02	C4 Ni1 O4	Tetracarbonyl-nickel	MX_4
FUZLUH	C12 Co4 O12 Sb4	tetrakis(Tricarbonyl-(M_3-stibido)-cobalt)	cuban
FUZTEZ	H16 B4 Np1	tetrakis(Tetrahydroborato)-neptunium(iv)	MX_4
FUZVOL	H16 B4 Hf1	tetrakis(Tetrahydroborato)-hafnium	MX_4
GERHOA	C4 H12 Cl12 N4 Sb4	1,3,5,7-Tetramethyl-2,2,2,4,4,4,6,6,6,8,8,8-dodecachloro-1,3,5,7 -tetra-aza-2,4,6,8-tetrastibapentacyclo(4.2.0.0^2, 5.0^3, 8.0^4, 7)octane	cuban
GUTCED	C26 H32	(1(2,3)4)Pentamantane	other
HMGETP	C12 H36 Ge6 P4	hexakis(Dimethylgermanium)tetraphosphide	adam
HMSIPA	C12 H36 P4 Si6	Dodecamethyl-hexasila-tetraphospha-adamantane	adam
HXMTAM07	C6 H12 N4	Hexamethylenetetramine	adam
JEYSEL	C18 H36 Ni4 O6 P4	hexakis(M_2-Carbonyl)-tetrakis(trimethylphosphine)-tetra-nickel	tetra
JUFWUC	C12 H40 Cs4 N4 Si4	tetrakis(M_3-Trimethylsilylamido)-tetra-cesium cubane	cuban
KANGUB01	C10 H12 I4	1,3,5,7-Tetraiodo-adamantane	adam
KELREY	C12 H36 Cl4 Ti4	tetrakis(M_3-Chloro)-tetrakis(trimethyl-titanium)	cuban
KOXKOX	C16 H36 Ga4 Se4	tetrakis((M_3-Selenido)-t-butyl-gallium)	cuban
KUJSIR	C20 H48 O4 Zn4	tetrakis(M_3-t-Butoxo)-tetrakis(methyl-zinc)	cuban
LUFYEQ	C12 H12 Si1	tetrakis(Prop-1-ynyl)silane	MX_4
MECKIO	C16 H36 Cl4 In4 N4	tetrakis(M_3-t-Butylimido)-tetrachloro-tetra-indium	cuban
MECKOU	C16 H36 Br4 In4 N4	tetrakis(M_3-t-Butylimido)-tetrabromo-tetra-indium	cuban
MECKUA	C16 H36 I4 In4 N4	tetrakis(M_3-t-Butylimido)-tetraiodo-tetra-indium	cuban
MESIAD	C12 H36 As4 Si6	Dodecamethyl-hexasila-tetra-arsa-adamantane	adam
MEZDIE01	C12 H36 Si1 Sn4	tetrakis(trimethylstannyl)silane	MX_4
MEZDOK01	C12 H36 Ge1 Sn4	tetrakis(trimethylstannyl)germane	MX_4

Identifier	formula	name
MPTHOT01	C12 H40 O4 Pt4	tetrakis((M3-Hydroxo)-trimethyl-platinum)
MSISUL10	C4 H12 S6 Si4	Tetra(methylsilicon)-hexasulfide
MTRETC10	C16 H12 O12 Re4 S4	tetrakis(Tricarbonyl-M3-methanethiolato-rhenium)
MXSNOX	C4 H12 O8 Sn6	tetrakis(M3-Methoxy)-tetrakis(M3-oxo)-hexa-tin
MZNMOX10	C8 H24 O4 Zn4	tetrakis((M3-Methoxo)-methyl-zinc)
NIWMIP	C12 H36 Al4 N4 S6	hexakis(M2-Sulfido)-tetrakis(trimethylamide)-tetra-aluminium
OHABEE	C16 H36 Si4	tetrakis(Trimethylsilyl)tetrahedrane
POSLOY10	C12 Cl4 O12 Tc4	tetrakis((M3-Chloro)-tricarbonyl-technetium)
QUGBOJ	C16 O16 Rh6	tetrakis(M3-Carbonyl)-dodecacarbonyl-hexa-rhodium
RASDOE	C16 H48 Ga4 N4 Si4	tetrakis(M3-Trimethylsilylimido)-tetramethyl-tetra-gallium(iii)
REKYUB	C16 H36 Ga4 S4	tetrakis((M3-Sulfido)-t-butyl-gallium)
RIMMOP	C16 H40 Al4 N4	tetrakis((M3-t-Butylamido)-hydrido-aluminium)
RIMNAC	C20 H48 Al4 N4	tetrakis((M3-t-Butylamido)-methyl-aluminium)
RUQMEV	C12 H36 Cu4 I4 N4	tetrakis(M3-Iodo)-tetrakis(trimethylamino)-tetra-copper(i)
SENLAY	C16 H36 P4 Si4	2,4,6,8-Tetra-t-butyl-1,3,5,7-tetraphospha-2,4,6,8-tetrasila-pentacyclo(4.2.0.0^{2}, 5.0^{3}, 8.0^{4}, 7)octane
TCYMET	C5 N4	Tetracyanomethane
TFMETH02	C1 F4	Carbon tetrafluoride
TMEPTC	C12 H36 Cl4 Pt4	tetrakis((M3-Chloro)-trimethyl-platinum)
TMGEHS10	C4 H12 Ge4 S6	Tetra(methyl-germanium) hexasulfide
TMSIAD	C10 H24 Si4	1,3,5,7-Tetramethyl-tetrasila-adamantane
TMSNHS10	C4 H12 S6 Sn4	Tetra(methyltin) hexasulfide
TOHSUE	C16 F12 O12 P4 Ru4	tetrakis((M3-Trifluoromethylphosphido)-tricarbonyl-ruthenium)
VADRAU	C4 H12 Pb1	Tetramethyl-lead(iv)
VAFWAA	C12 Bi4 Co4 O12	tetrakis(Tricarbonyl-(M3-bismuth)-(M3-cobalt))
VAVYAS	C20 H36 P4	2,4,6,8-Tetra-t-butyl-1,3,5,7-tetraphosphacubane
XAGXAE	P4 S10	2,4,6,8,9,10-Hexathia-1,3,5,7-tetraphosphatricyclo(3.3.1.1^{3}, 7)decane 1,3,5,7-tetrasulfide
XUWROW	C20 H48 Mg4 O4	tetrakis(M3-t-Butoxo)-tetramethyl-tetra-magnesium
YEMRIR	O6 P4 S4	2,4,6,8,9,10-Hexaoxa-1,3,5,7-tetraphosphatricyclo(3.3.1.1^{3}, 7)decane 1,3,5,7-tetrasulfide
YEYQAU	C12 O12 Ru4 Se4	tetrakis((M3-Selenido)-tricarbonyl-ruthenium)
YIMWEW	C10 H16 O4	1,3,5,7-Tetrahydroxyadamantane
ZEYHIU	C20 H48 Cd4 O4	tetrakis((M3-t-Butoxo)-methyl-cadmium)
ZIZHIZ	C12 H4 Mn4 O16	tetrakis((M3-Hydroxo)-tricarbonyl-manganese)
ZNOXAC01	C12 H18 O13 Zn4	hexakis(M2-Acetato-O,O')-(M4-oxo)-tetra-zinc
ZZZKDW01	C1 I4	Carbon tetraiodide

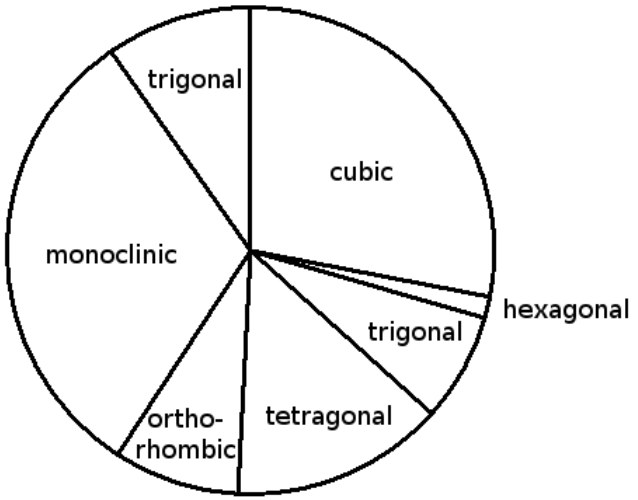

FIG. 1: Crystal systems for crystals of tetrahedral molecules.

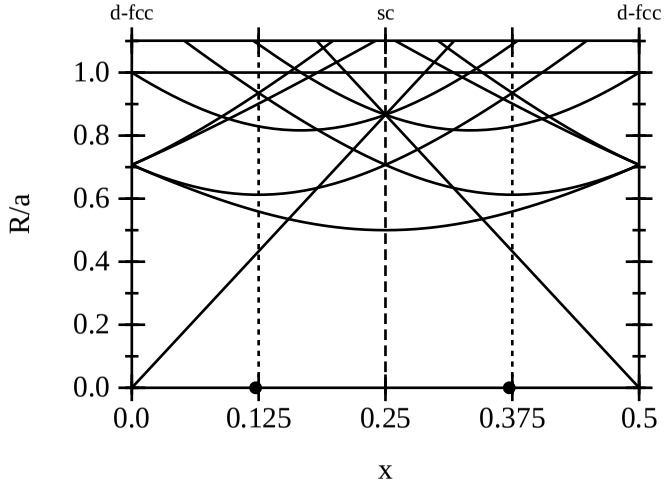

FIG. 2: Neighbor distances for 205c as a function of the Wyckoff structural parameter, x. The

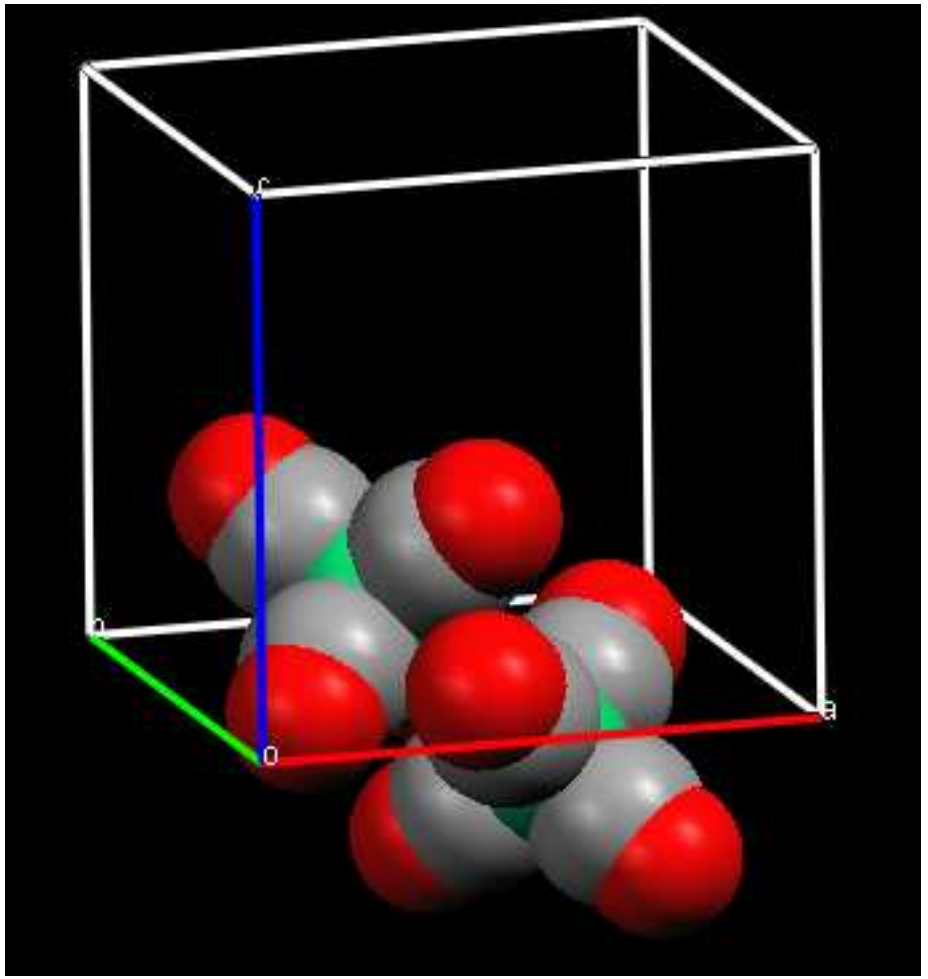

FIG. 3: Crystal structure of tetracarbonyl-nickel [CSD structure FOJBUB02 [24]] in space group 205c with molecules at Wyckoff point c. It is a fcc lattice of dimers at Wyckoff point a as shown for one dimer centered at fractional coordinate $(1/2, 1/2, 0)$.

TABLE III: Reference lattices for hexagonal and trigonal structures. Ideal reference lattice parameters and Wyckoff structural parameters are listed below the experimental data.

Structure	Example Lattice	c/a	Str. Param's	$\|G\|/Z$	Entries
165d	DILWIE01	3.07	z=0.122	3	2
	hcp	3.27	z=1/8	12	
161a	TCYMET	1.28	z=0.000	3	1
	bcc	1.22	z=0	48	
147d	ZIZHIZ	1.51	z=0.252	3	1
	hcp	1.63	z=1/4	12	
176h	CUCZUV	0.89	x=0.361, y=0.334	2	1
	hcp	0.94	x=1/3, y=1/3	12	
152b	MTRETC10	2.57	x=0.715	2	1
	fcc	2.45	x=2/3	48	
				total:	6

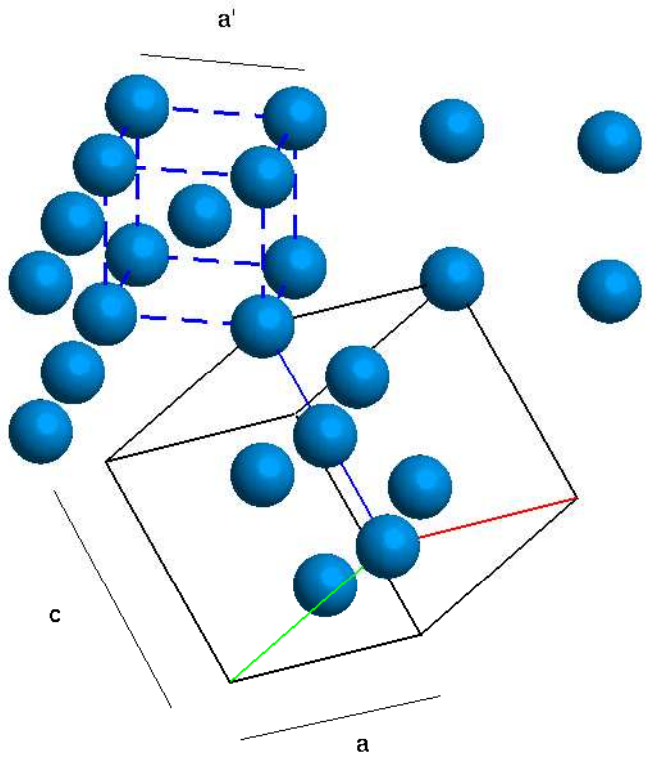

FIG. 4: The crystal structure of TCYMET embedded in a bcc reference lattice. The molecular centers of mass are depicted as spheres. The lattice constant of the bcc reference lattice, a', is compared to the lattice constants a and c of TCYMET.

TABLE IV: Reference lattices for tetragonal structures

Structure	Example Lattice	c/a	Str. Parameters	$\|G\|/Z$	Entries
141a	FUZLUH	0.72		8	2
	A5′	0.76		8	
137b	FUZTEZ	0.70		8	1
	Aa	0.82		16	
121a	ZZZKDW01	1.49		8	1
	fcc	1.41		48	
142a	KUJSIR	2.02		4	1
	fcc	2.00		48	
120c	YEMRIR	1.50		4	1
	sc	1.41		48	
114a	ADAMAN08	1.34		4	2
	fcc	1.41		48	
88a	KANGUB01	3.97		4	1
	A5″	3.46		8	
88f	LUFYEQ	1.25	z=0.311	1	1
	d-Aa∗	1.15	z=3/8	8	
				total:	10

* dimer packing

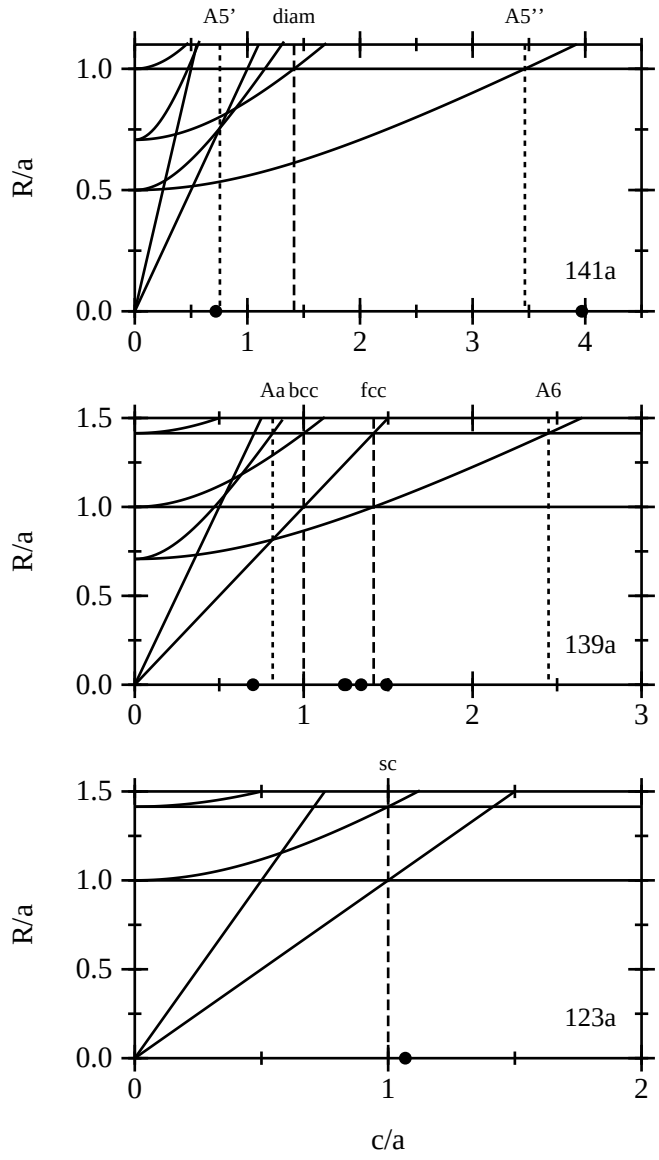

FIG. 5: Neighbor distances for 141a, 139a, and 123a as a function of the c/a ratio. The tetragonal distortions include diam, bcc, fcc, and sc as special cases. Experimental values are marked with circles. Additional neighbors are omitted for clarity at small c/a values.

TABLE V: Reference lattices for orthorhombic structures

Structure	Example Lattice	b/a	c/a	Str. Parameters	$\|G\|/Z$	Entries
62c	GUTCED	1.10	1.09	x=0.171, z=-0.014	2	1
	fcc	1.00	1.00	x=1/4, z=0	48	
62c	RIMMOP	1.46	1.61	x=0.187, z=0.032	2	1
	bcc	1.41	1.41	x=1/4, z=0	48	
62c	JEYSEL	1.62	1.80	x=-0.069, z=-0.030	2	1
	sh	1.63	1.73	x=0, z=0	24	
64d,f	METHANEIII	0.70	0.70	x=0.250	1	1
				y=0.230, z=0.270		
	fcc	0.71	0.71	x=1/4	48	
				y=1/4, z=1/4		
19a	MZNMOX10	1.03	3.93	x=-0.066, y=0.067, z=0.123	1	1
	63c	1.00	3.15	x=0, y=0, z=0.112	4	
60c,d	YIMWEW	0.45	0.46	y=-0.188	2/3	1
				x=0.169, y=0.297, z=0.206		
	bcc	0.47	0.47	y=-1/4	48	
				x=1/6, y=1/4, z=1/4		
					total:	6

TABLE VI: Reference lattices for monoclinic structures

Structure	Example Lattice	b/a	c/a	β	Str. Parameters	$\lvert G\rvert/Z$	Entries
15e	REKYUB	0.48	1.00	123	y=-0.024	2	3
	fcc	0.58	1.16	125	y=0	48	
15e	RASDOE	0.51	0.97	120	y=0.123	2	1
	70a	0.50	1.00	120	y=1/8	4	
15e	TMGEHS10	1.78	1.14	108	y=0.106	2	3
	A5′	1.87	1.06	118	y=1/8	8	
12i	MECKOU	0.73	1.17	110	x=0.253, z=0.241	2	1
	fcc	0.58	1.00	109	x=1/4, z=1/4	48	
11e	MECKIO	1.61	1.13	105	x=0.205, y=0.219	2	1
	bcc	1.63	1.00	109	x=1/4, y=1/4	48	
14e	TOHSUE	1.01	2.76	90	x=0.250, y=0.745, z=0.126	1	1
	fcc	1.00	2.83	90	x=1/4, y=3/4, z=1/8	48	
14e	TMSIAD	1.11	2.07	91		1	1
	d-sh∗	1.22	2.12	90		12	
14e	CAMPOV	1.41	1.64	92		1	2
	d-sc∗	1.41	1.41	90		24	
14e	DOCNIS	1.45	1.80	60	x=0.102, y=0.255, z=0.072	1	1
	hcp	1.63	2.00	60	x=1/6, y=1/4, z=1/12	12	
14e	CARBTC	0.63	1.01	104	x=0.248, y=0.067, z=0.157	1	1
	hcp	0.61	1.06	90	x=1/4, y=0, z=1/6	12	
14e	QUGBOJ	0.59	1.06	105	x=0.268, y=0.129, z=0.070	1	1
	A5′	0.76	1.00	90	x=1/4, y=1/8, z=0	8	

∗ dimer packing

Structure	Example	b/a	c/a	β	Str. Parameters	$\lvert G\rvert/Z$	Entries
	Lattice						
14e	MECKUA	0.66	1.14	113	x=0.501, y=0.225, z=0.749	1	1
	fcc	0.59	1.00	109	x=1/2, y=1/4, z=3/4	48	
14e,e	CANFIG	0.92	1.10	26	x=0.331, y=0.340, z=0.005	1/2	1
	d-136∗	1.00	1.12	27	x=1/3, y=1/3, z=0	2	
14e,e	MXSNOX	1.76	1.74	75		1/2	1
	d-sh∗	1.73	1.91	59		12	
13e,f,g	RIMNAC	0.52	1.84	94	y=0.480	1/2	1
					y=0.813		
					x=0.256, y=0.158, z=0.001		
	70a	0.50	1.73	90	y=3/8	4	
					y=5/8		
					x=1/4, y=1/8, z=0		
15f,f,f,f	CTBROM	0.57	0.98	111	x=0.096, y=0.032, z=0.378	1/4	2
					x=0.379, y=0.060, z=0.120		
					x=0.126, y=0.316, z=0.123		
					x=0.345, y=0.291, z=0.371		
	fcc	0.58	1.00	109	x=1/8, y=0, z=3/8	48	
					x=3/8, y=0, z=1/8		
					x=1/8, y=1/4, z=1/8		
					x=3/8, y=1/4, z=3/8		
						total:	22

∗ dimer packing

TABLE VII: Reference lattices for triclinic structures

Structure	Example Lattice	b/a	c/a	α	β	γ	Str. Parameters	$\|G\|/Z$	Entr
2i	BASXOI	1.15	1.15	86	90	66	x=0.297, y=0.306, z=0.299	1	1
	A6	1.00	1.00	90	90	60	x=1/4, y=1/4, z=1/4	16	
2i	XAGXAE	1.02	1.02	93	101	110		1	1
	d-Ai*	1.15	0.83	87	97	116		6	
2i	XUWROW								-
	epitaxial crystal—70% voids								
2i	MEZDIE01	1.46	0.92	90	112	90	x=0.261, y=0.251, z=0.242	1	2
	bcc	1.63	1.00	90	109	90	x=3/4, y=1/4, z=1/4	48	
2i,i,i	OHABEE	1.49	2.57	90	90	90	x=0.320, y=0.247, z=0.585	1/3	1
							x=0.016, y=0.254, z=0.250		
							x=0.318, y=0.754, z=0.082		
	bcc	1.63	2.83	90	90	90	x=1/3, y=1/4, z=7/12	48	
							x=0, y=1/4, z=1/4		
							x=1/3, y=3/4, z=1/12		
2i,i,i,i	CANFOM	0.92	0.48	88	91	88	x=0.162, y=0.842, z=0.484	1/4	1
							x=0.334, y=0.340, z=-0.008		
	d-136*	1.00	0.50	90	90	90	x=1/6, y=5/6, z=1/2	2	
							x=1/3, y=1/3, z=0		
								total:	7

* dimer packing

TABLE VIII: Summary of reference lattices inferred from experimental data.

Struktur-bericht	Pearson Symbol	Common Name	Space Group	Wyckoff Point(s)	$\|G\|/Z$	Comments	Monomer Structures	Dimer Structures
A2	cI2	bcc	229	a	48	sphere packing	18	
A1	cF4	fcc	225	a or b	48	sphere packing	15	2
Ah	cP1	sc	221	a or b	48	sphere packing	4	2
A3	hP2	hcp	194	c or d	12	sphere packing	6	
A5′	tI4		141	a or b	8	distorted diamond with c/a=$2/\sqrt{7}$	6	
Af	hP1	sh	191	a	24	simple hexagonal	1	2
A15	cP8		223	a and (c or d)	6	least-area structure	3	
Aa	tI2	bct	139	a or b	16	distorted bcc with c/a=$\sqrt{2}/3$	1	1
	tP8		136	f,f	8	dimer packing		2
	oF8		70	a	4		2	
A4	cF8	diamond	227	a or b	24	sphere packing	1	
Ai	tR2		166	a,a	18	dimer packing		1
A6	tI2	fct	139	a or b	16	distorted fcc with c/a=$\sqrt{6}$	1	
A5″	tI4		141	a or b	8	distorted diamond with c/a=$2\sqrt{3}$	1	
	oC2		63	c	8		1	

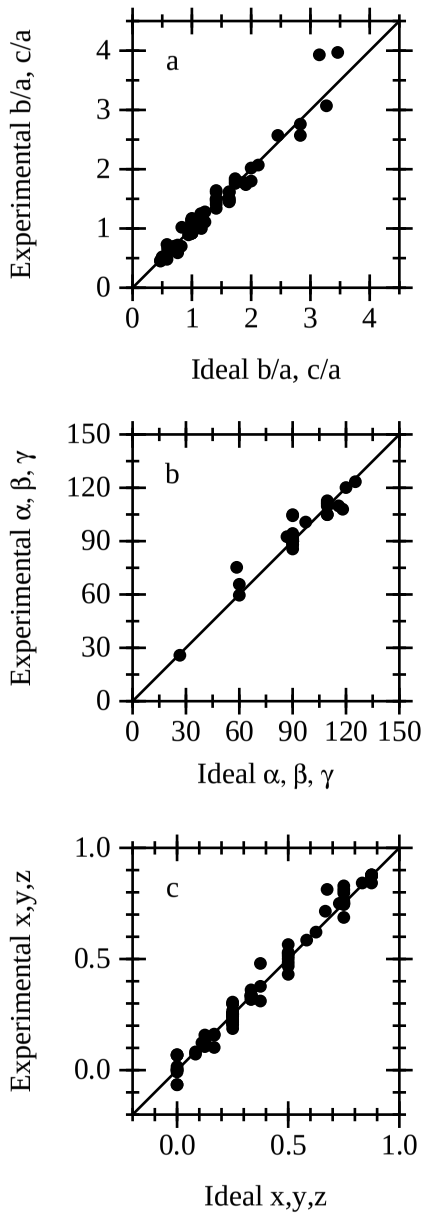

FIG. 6: Comparison of experimental and ideal reference (a) lattice lengths, (b) angles, and (c) structural parameters. The 45-degree line indicates perfect agreement between the experimental

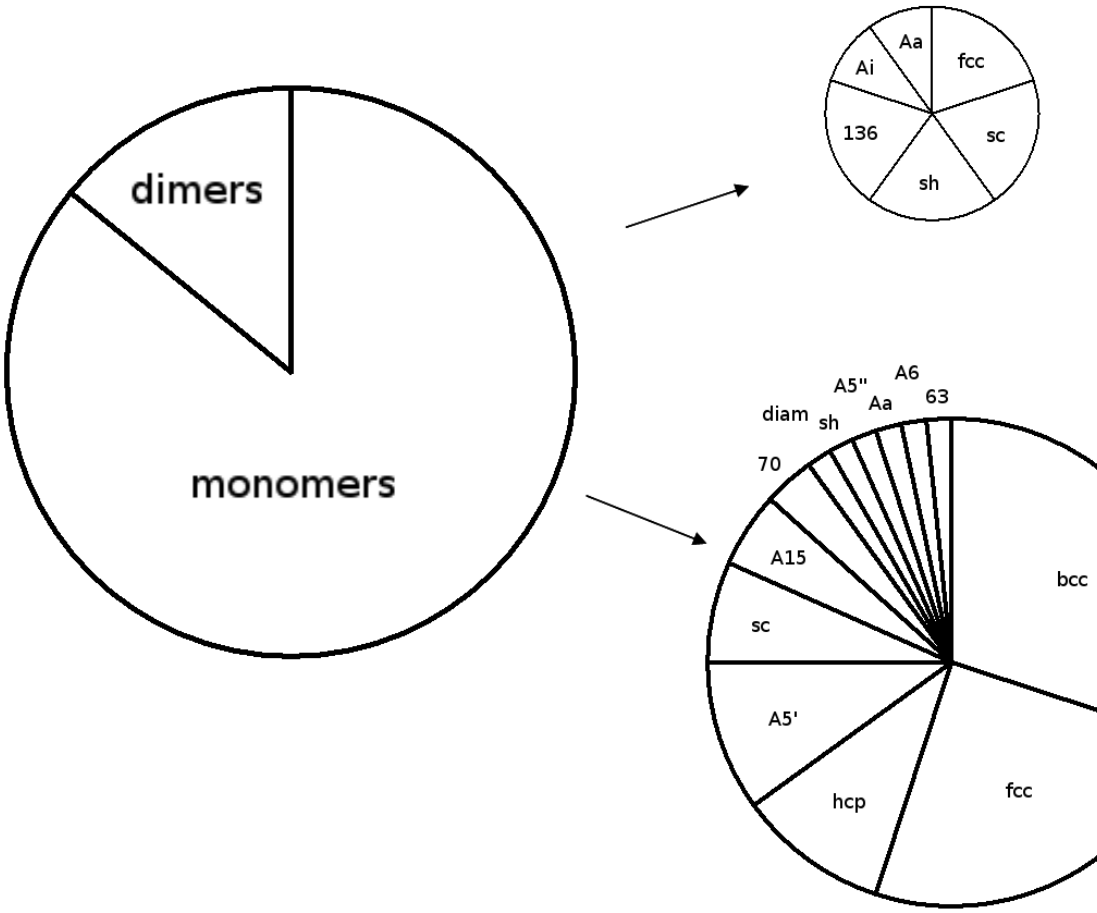

FIG. 7: Relative proportions of monomer and dimer structures in the experimental data set and refer

TABLE IX: Dimer complexes among crystals of tetrahedral molecules.

structure	dimer Wyck. Pt.	representative entry	reference lattice	point-group symmetry	entries
205c	a	FOJBUB02	d-fcc	D_{3d}	2
88f	e	LUFYEQ	d-Aa	C_{2v}	1
14e	a	TMSIAD	d-sh	C_i ($\sim D_{3d}$)	1
14e	a	CAMPOV	d-sc	C_i ($\sim D_{3d}$)	2
14e,e	e	CANFIG	d-136	C_1 ($\sim D_{3d}$)	1
14e,e	b,c	MXSNOX	d-sh	C_i ($\sim D_{3d}$)	1
2i	a	XAGXAE	d-166	D_{3d}	1
2i,i,i,i	i,i	CANFOM	d-136	C_1 ($\sim D_{3d}$)	1
				total:	10

Note: Point group symmetries were assigned by visual inspection.